**A $\nu-$gap Factsheet**
**–with Applications to Model Validation–**

Wolfgang Reinelt

Department of Electrical Engineering
Linköping University, 581 83 Linköping, Sweden
WWW: http://www.control.isy.liu.se/~wolle
Email: wolle@isy.liu.se

May 2001

REGLERTEKNIK
AUTOMATIC CONTROL
LINKÖPING

Report no.: LiTH-ISY-R-2354

# A $\nu-$gap Factsheet –with Applications to Model Validation–

Wolfgang Reinelt

Division of Automatic Control, Dept of Electrical Engineering,
Linköping University, 581 83 Linköping, Sweden.
wolle@isy.liu.se, http://www.control.isy.liu.se/~wolle

**Abstract**

Typical measures for closed loop systems are so-called *gaps* between two systems, classically either $\mathcal{L}_2$ or $\mathcal{H}_2$ gap. Here, the distance between to candidate models for a plant can be measured taking all possible combinations of bounded input and output signals into account. Rather recently, a variant of theses gaps, the $\nu-$gap, gained interest in the "identification for control" community. This report states the basic technicalities of this framework along with a motivation, why a new gap is useful. Moreover, the possibilities of examining models set, arising from an identification experiment, in terms of this metric are discussed. Some simple examples are given to illustrate the framework.

*Keywords: $\nu$-gap, coprime factors, gap-metric.*

## 1 Introduction and motivation

Typical measures for closed loop systems are *gaps* between two systems, classically either $\mathcal{L}_2$ or $\mathcal{H}_2$ gap. Here, the distance between to candidate models for a plant can be measured taking all possible combinations of bounded input and output signals into account. Rather recently, a variant of theses gaps, the $\nu-$gap [23, 25], gained interest in the "identification for control" community, especially for analysis or validation of (identified) model sets with respect to robust stability of a given controller. However, the roots of $\nu-$gap are somewhat different, namely to "repair" some shortcomings in the $\mathcal{L}_2$ or $\mathcal{H}_2$ gaps: robustness and computability issues. Indeed, $\nu-$gap turns out to be the $\mathcal{L}_2$ gap with some "built in" Nyquist criterion in order to account for sharp stability and robustness results. We will motivate the introduction from this perspective. This forces us to repeat some basic facts on the framework of coprime factors, which is well-established and ancient history (=mid 1980's) in $\mathcal{H}_\infty$ theory. The exposition here, however, is not aimed at starting from a zero level. For an "introduction by example", we recommend to study Chapter 12 of [11]. For a complete run through all the maths required we refer to the standard reference [14] (containing some examples as well), or the respective chapters on coprime factors and $\mathcal{H}_\infty$ Loop Shaping in [26, 27]. A very classical reference on this material is the book by Vidyasagar [20].

This report is basically the outcome of a couple of seminars and talks, given on this subject, and some numerical experimentation and is intended to sum up these

**Outline:** This report is organised as follows: Sec. 2 states the basic features of the coprime factor framework. Motivated by that, Sec. 4 defined the usual gap-metrics and the $\nu-$gap-metric. These results are then applied to analysing/validating sets of (identified) models with respect to stability of a *given* controller, along with an extensive example. Sec. 5 gives some remarks on future directions of $\nu -$ gap.

## 2 Recap: coprime factors and robust stability

**Definition 1 (Function spaces and $\infty$-Norm)** *Just to get the notation, we state some abbreviations here. For some more accurate equations, see the "signals and systems" chapter in any textbook on linear control theory, for instance [11].*

*The $\infty$-norm of a transfer-function matrix $G$ is given by*

$$||G||_\infty \quad := \quad \sup_\omega \overline{\sigma}\left(G(i\omega)\right)$$

*(whenever this expression this exists) where $\overline{\sigma}(\cdot)$ denotes the maximum singular value.*

*$\mathcal{RL}_\infty$ denotes the space of all transfer-function matrices with finite $\infty$-norm, while $\mathcal{RH}_\infty$ denotes the space of all transfer-function matrices in $\mathcal{RL}_\infty$ with no poles in $Re(s) > 0$. Because we only work with real-rational transfer-function, we often write $\mathcal{H}_\infty$ instead of $\mathcal{RH}_\infty$.*

*Let $\mathcal{L}_2$ be the space of signals with bounded energy and support $-\infty < t < \infty$. Let $\mathcal{H}_2$ be the space of signals with bounded energy and support $0 \leq t < \infty$ .*

We now quickly derive the notion of coprime factors with only a few definitions, see [14] for details. It is aimed to represent *any* LTI systems by just stable "components".

**Definition 2 (Left-Coprime)** *$M, N \in \mathcal{RH}_\infty$ and $M, N$ have the same number of rows. Then $M$ and $N$ are called left-coprime iff $U, V \in \mathcal{RH}_\infty$ exist such that the* Bezout-identity *holds:*

$$MV - NU \quad = \quad I$$

**Definition 3 (Left-Coprime Factorisation, LCF)** *The pair $(M, N)$ with $M, N \in \mathcal{RH}_\infty$ constitute a left-coprime factorisation (LCF) of $G \in \mathcal{R}$ iff*

1. *$M$ square and nonsingular*
2. *$G = M^{-1}N$*
3. *$M$ and $N$ are left-coprime.*

**Definition 4 (Normalised Left-Coprime Factorisation, NLCF)** *The pair $(M, N)$ with $M, N \in \mathcal{RH}_\infty$ constitute a normalised left-coprime factorisation (LCF) of $G \in \mathcal{R}$ iff*

1. *$(M, N)$ is a LCF of $G$*
2. *$NN^* + MM^* = I \quad \forall s = i\omega, \omega \in \mathbb{R}$*

**Remark 1** *The normalised coprime factors of a given transfer function $G$ can be computed via state-space formulas. They depend on a minimal state-space representation $(A, B, C, D)$ of $G$ – see [14, section 2.5.2] for details.*

If the coprime factorisation of the plant is known, the error can be modelled as an error of the coprime factors (see Figure 1). This approach has several advantages: the number of unstable poles of the uncertain plant need not be equal to those of the nominal plant, the error bounds of the coprime factors can be chosen smaller than those of e.g. a multiplicative error. An important advantage is the stability of all participated "components": numerator, denominator and their errors are stable even if the plant is unstable. The bounds are given by the operator- ($\mathcal{H}_\infty$-) norm:

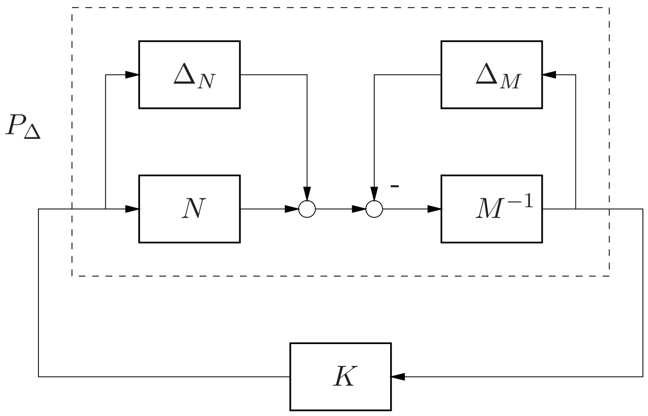


Figure 1: Normalised coprime factorisation: $K$ stabilises $P = M^{-1}N$.

**Definition 5 (Description of the model uncertainty)** *Let $P = M^{-1}N$ and $P_\Delta$ be the transfer function of the nominal and the perturbed plant respectively. The uncertainty can be modelled as an error of the coprime factors (see Figure 1):*

$$P_\Delta = (M + \Delta_M)^{-1}(N + \Delta_N). \tag{1}$$

**Definition 6 (Admissible Perturbation)** *For $\epsilon > 0$ a perturbation $\Delta = [\Delta_N, \Delta_M]$ of a transfer function as described in 5 is called ($\epsilon$-)admissible, when $||\Delta||_\infty < \epsilon$ holds. The set of all ($\epsilon$-)admissible perturbations is denoted by $\mathcal{D}_\epsilon$:*

$$\mathcal{D}_\epsilon := \{\Delta : \Delta \in \mathcal{RH}_\infty; ||\Delta||_\infty < \epsilon\} \tag{2}$$

Having this definition of nominal model and uncertain model at hand, we arrive at the following main result, which we would like to discuss deeper:

**Theorem 1 (Robust Stabilisation)** *$K$ stabilises the uncertain plant $P_\Delta = (M + \Delta_M)^{-1}(N + \Delta_N)$ (in Fig. 1) for all $\Delta = [\Delta_N, \Delta_M] \in \mathcal{D}_\epsilon$ iff*

1. *$K$ stabilises $P$*
2. *the following equation holds:*

$$\left|\left|\left[\begin{array}{c} K(I - PK)^{-1}M^{-1} \\ (I - PK)^{-1}M^{-1} \end{array}\right]\right|\right|_\infty \leq 1/\epsilon \tag{3}$$

It it clear from the robust stabilisation Theorem 1, that we are searching the largest positive number $\epsilon (= \epsilon_{\max})$, which fulfils (3). In this case, we will have "maximal robustness". One of the beauties of this approach is now, that this so-called maximum stability margin can be obtained in a surprisingly explicit manner: no binary search, as for instance in the case of $\mathcal{H}_\infty$ closed loop shaping is required to arrive at the optimal value.

**Corollary 1** *NLCF Robust Stabilisation Problem Let $(N, M)$ the NLCF of the plant $P$. Then, the largest positive number $\epsilon (= \epsilon_{\max})$ such that $P_\Delta = (M + \Delta_M)^{-1}(N + \Delta_N)$ can be stabilised by a single controller $K$ for all $\Delta \in \mathcal{D}_\epsilon$ is given by*

$$\epsilon_{\max} = 1/\gamma_{\min} = \left( \inf_{stab\, K} \left|\left|\left[\begin{array}{c} K \\ I \end{array}\right](I - PK)^{-1}M^{-1}\right|\right|_\infty \right)^{-1} = \sqrt{1 - ||[N, M]||_H^2} \tag{4}$$

*where $|| \cdot ||_H$ denotes the so-called Hankel norm.*

Now, the question popping up is: what about the "big uncertainties" with $||\Delta||_\infty \geq \epsilon$? To see, that the above Theorem does not answer this question, it is more convenient to look at the negation of Theorem 1:

**Corollary 2** *There exists an admissible $P_\Delta$ so that the closed loop $[K, P_\Delta]$ is unstable if and only if*

$$\left|\left|\left[\begin{array}{c} K(I-PK)^{-1}M^{-1} \\ (I-PK)^{-1}M^{-1} \end{array}\right]\right|\right|_\infty^{-1} < \epsilon.$$

So, what do we learn about the "big uncertainties" with $||\Delta||_\infty \geq \epsilon$ from the two results stated above? Not that much, at least not for *all* these $\Delta's$ (technically speaking, the term $\Delta$ is in the "wrong" position of the equivalence, preventing a statement for all $\Delta's$). What we want to have is a somewhat stronger result, that holds for all "big" uncertainties. This is a problem of the metric, in which the distance between two systems is measured. The induced topology is obviously not the one that separates the stabilisable plants from the unstabilisable one, which brings $\nu-$gap onto the stage: let's design a metric, so that the induced topology is better fitted for stability questions.

Before doing this, it is motivated to pause and think about we can expect. Well, what we can *not* expect is a result like: all control lops $[K, P_\Delta]$ made up with a $||\Delta||_\infty \geq \epsilon$ are *always* unstable (with the above controller). Why not? This would mean that the set of stabilisable uncertainties may be described *exactly* in terms of the $\infty$-norm on $\Delta$, i.e. in the $\mathcal{H}_2$-gap (which is not true).

In the MIMO case, one can increase the set of "allowed" uncertainties by employing ellipsoids instead of circles around the nominal coprime factors, which basically means scaling the singular values with different weights. This leads to the term of *multi-directional optimal robustness* [17], see also Fig. 2.

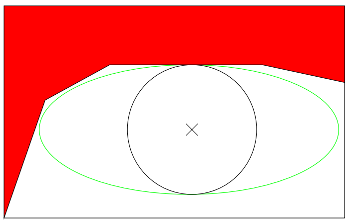

Figure 2: Multi-directional optimal robustness (P.-O. Nyman). Suppose, the centre of the ellipsoid is the nominal system, say, $P$, along with a stabilising controller. Suppose, the shaded area is the subset of plants that *cannot* be stabilised with this controller Now, we are desperately interested in how far (in some measure) we can "move" away from $P$ and still having a stable control system. Then, measuring in ellipsoids instead of balls we certainly cover a bigger part of the plants that can be stabilised.

# 3 $\nu$ – gap: definition and stability results

## 3.1 Some mathematical preliminaries

In order to state the somewhat sharper stability result in the face of plant uncertainty, we need to give a couple of definitions first.

**Definition 7 (Graph and graph symbol)** *Define the **graph and the graph symbol** as follows*

- *Let* $L_p : \mathcal{L}_2 \to \mathcal{L}_2, u \to Pu$. *Then*

$$\mathcal{G}(L_p) := \left\{ \begin{pmatrix} Pu \\ u \end{pmatrix} ; u \in \mathcal{L}_2, Pu \in \mathcal{L}_2 \right\}$$

  *is called the* $\mathcal{L}_2$*-graph.*

- *Let* $M_p : \mathcal{H}_2 \to \mathcal{H}_2, u \to Pu$. *Then*

$$\mathcal{G}(M_p) := \left\{ \begin{pmatrix} Pu \\ u \end{pmatrix} ; u \in \mathcal{H}_2, Pu \in \mathcal{H}_2 \right\}$$

  *is called the* $\mathcal{H}_2$*-graph.*

- *Let* $P = NM^{-1}$ *be a normalised right coprime factorisation of* $P$ *and* $G := \begin{pmatrix} N \\ M \end{pmatrix}$. *Then*

$$\mathcal{G} := \mathcal{G}(M_p) = G \cdot \mathcal{H}_2$$

  *is called the graph symbol.*

In the following, we are about to measure distance between dynamic systems. In order to motivate the following derivations, we first start an attempt with the "usual" $\mathcal{H}_\infty$ norm. This is to define a metric on $\mathcal{RH}_\infty$ as follows

$$\delta_n(P_1, P_2) := \sup_{u \in \mathcal{H}_2, u \neq 0} \frac{||P_1 u - P_2 u||_2}{||u||_2}$$

What is wrong with that? Well, employing $\delta_n$ as a measure between plants (to be controlled) from a "closed loop point of view" we notice that $\delta_n$ assumes *equal* input to both plants $P_1$ and $P_2$, which is not true in feedback situation, cf. Fig. 3. Considering this, it might be better to compare something like

$$\frac{\left|\left| \begin{pmatrix} y_1 \\ u_1 \end{pmatrix} - \begin{pmatrix} y_2 \\ u_2 \end{pmatrix} \right|\right|_2}{\left|\left| \begin{pmatrix} y_1 \\ u_1 \end{pmatrix} \right|\right|_2}.$$

Extremely motivated by this simple observation, we define the following, rather complicated looking, object:

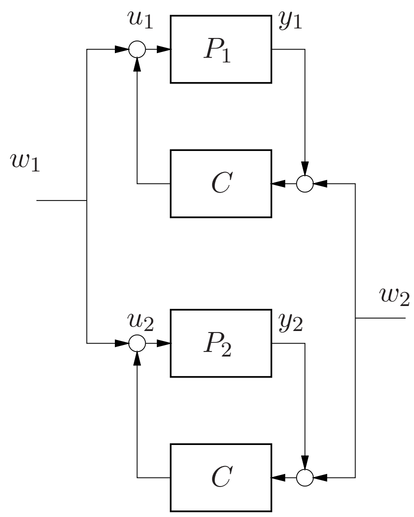


Figure 3: uncertainty in feedback situation.

**Definition 8 (Directed $\mathcal{H}_2$-gap and $\mathcal{H}_2$-gap metric)** *Define the directed gap:*

$$\vec{\delta}_g(P_1, P_2) \quad := \quad \sup_{\begin{pmatrix} u_1 \\ y_1 \end{pmatrix} \in \mathcal{G}_1} \; \inf_{\begin{pmatrix} u_2 \\ y_2 \end{pmatrix} \in \mathcal{G}_2} \frac{\left\| \begin{pmatrix} y_1 \\ u_1 \end{pmatrix} - \begin{pmatrix} y_2 \\ u_2 \end{pmatrix} \right\|_2}{\left\| \begin{pmatrix} y_1 \\ u_1 \end{pmatrix} \right\|_2}$$

**Theorem 2 (short, but highly non-trivial!)**

$$\vec{\delta}_g(P_1, P_2) = \inf_{Q \in \mathcal{H}_\infty} ||G_1 - G_2 Q||_\infty$$

*and the symmetrised version of $\vec{\delta}_g$ is a metric:* $\delta_g(P_1, P_2) := \max \left\{ \vec{\delta}_g(P_1, P_2), \vec{\delta}_g(P_2, P_1) \right\}$.

**Remark 2** *Indeed, $\delta_g$ is the metric used in the coprime factor framework of Sec. 2, where it was quite easy to compute (although it looks quite messy here). In general, it is* not at all *easy to calculate.*

Applying the same reasoning (i.e. apply definition of "distance" between subspaces of Hilbert spaces) to $\mathcal{L}_2$-graph instead of $\mathcal{H}_2$-graph, we obtain the $\mathcal{L}_2$-gap metric:

$$\delta_{\mathcal{L}_2}(P_1, P_2) = ||(I + P_2 P_2^*)^{-1/2}(P_2 - P_1)(I + P_1 P_1^*)^{-1/2}||_\infty$$

This, however, may be calculated quite easily using the frequency response. Unfortunately, it does not take care of right half plane pole/zero constellations and is therefore not useful for deriving (robust) stability results. What we are looking for is in-fact a metric, allowing robust stability results *and* being easy to compute. This is $\nu -$ gap!

### 3.2 What the crowd is waiting for: the $\nu -$ gap metric

As motivated by the above derivations, $\nu -$ gap is loosely speaking the $\mathcal{L}_2$-gap plus some "built-in" stability criterion. Let's state the definition:

**Definition 9 ($\nu -$ gap metric)** *Define the $\nu -$ gap metric between two systems as follows:*

$$\delta_\nu(P_1, P_2) := \begin{cases} ||\tilde{G}_2^* G_1||_\infty & det(\tilde{G}_2^* G_1)(i\omega) \neq 0 \\ & \text{and } wnodet(\tilde{G}_2^* G_1) = 0 \\ 1 & \text{otherwise} \end{cases}$$

*where $G_i$ are the graph symbols for a NRCF of $P_i$, $\tilde{G}_i$ graph symbol for NLCF of $P_i$ and*

$$wnodet(\tilde{G}_2^* G_1) = wnodet(I + P_2^* P_1) + \eta(P_1) + \eta(P_2),$$

*where the winding number wno is evaluated along the standard Nyquist contour and $\eta(\cdot)$ denotes the number of unstable poles.*

**Remark 3** $||\tilde{G}_2^* G_1||_\infty = ||(I + P_2 P_2^*)^{-1/2}(P_2 - P_1)(I + P_1 P_1^*)^{-1/2}||_\infty$ *is the same expression as for the $\mathcal{L}_2$-gap.*

It may not be that straightforward to see, that the object defined above actually is a *metric*. The proof therefore is given in [23]. In the single-input single-output case, $\nu -$ gap allows a nice graphical interpretation and an easy numerical solution. It is shown in [23], that in-fact no frequency sweep is necessary but the $\nu -$ gap between two LTI plants can be calculated by their state space representations (for instance implemented in Matlab's $\mu$ analysis toolbox: `nugap`). Moreover, the SISO case leads us to the so-called *chordal distance* as well.

**Remark 4 ($\nu -$ gap: SISO case and chordal distance)** *If the winding number condition is fulfilled, $\nu -$ gap is the supremum over all frequencies ($s = i\omega$) of the so-called chordal distance $\kappa$ between two systems:*

$$\delta_\nu(P_1, P_2) = \max_\omega \kappa(P_1(i\omega), P_2(i\omega)); \ \kappa(x, y) = \frac{|x - y|}{\sqrt{1 + |x|^2}\sqrt{1 + |y|^2}}.$$

*A possible interpretation can be given by projection onto Riemann sphere, cf. Fig. 4. Hence, $\nu -$ gap can be seen as a sort of "normalised" $\mathcal{H}_\infty$ norm with a built in Nyquist criterion.*

After a quick definition of the *stability margin*, which we implicitly used in Sec. 2, we turn to the advertised result, i.e. robust stability, measured with $\nu -$ gap.

**Definition 10 (Stability margin)** *Define the stability margin as*

$$b_{K,P} = \inf_\omega \underline{\sigma}(\tilde{C}G)(i\omega),$$

*where $\tilde{C}, G$ denote the graph symbols for $K, P$.*

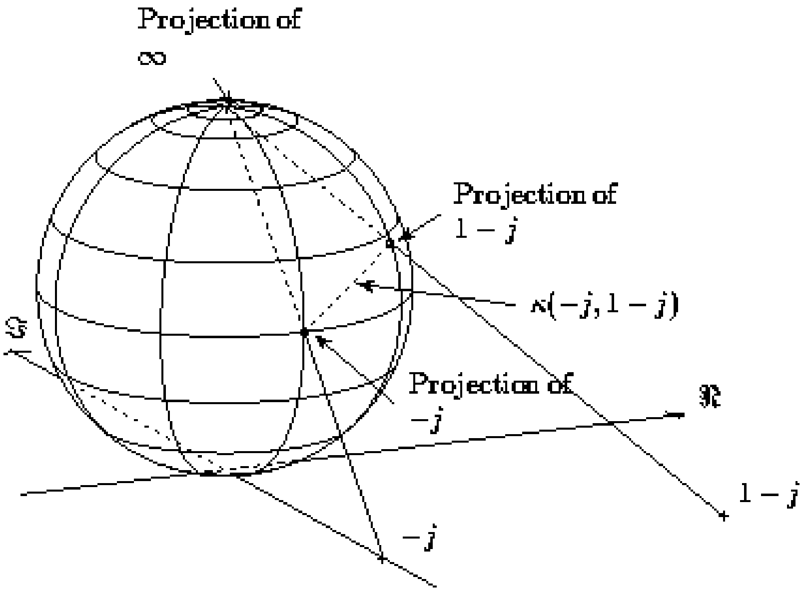


Figure 4: $\nu-$gap and projection onto Riemann sphere. (Figure V.10 from [22])

As a first result, we obtain the same result as for coprime factor framework using the $\mathcal{H}_2$-gap:

**Theorem 3 (Robust stability measured with $\nu-$gap)** *Given nominal plant $P$, compensator $K$ and a scalar $\beta$, then:*

$$[K, P_\Delta] \text{ stable for all } \delta_\nu(P, P_\Delta) \leq \beta \text{ iff: } b_{K,P} > \beta$$

We finally state the stronger result (which can *not* be obtained using the $\mathcal{H}_2$-gap), i.e. if the perturbed plant is "too far" away, then there is a compensator that stabilises the nominal plant, but not the perturbed one. This really the major result we gain in this approach!

**Theorem 4 (Robust stability measured with $\nu-$gap, second service)** *Given nominal plant $P$, perturbed plant $P_\Delta$ and a scalar $\beta$, then:*

$$[K, P_\Delta] \text{ stable for all compensators } K \text{ with } b_{K,P} > \beta \text{ iff } \delta_\nu(P, P_\Delta) \leq \beta$$

Those, interested in some more equations and state-space realisations are referred to Chapter 13 of [26] or the original references by Vi$\nu\nu$icombe [21, 22, 25].

### 3.3 Example

To see the difference between measuring the difference between systems in an open loop fashion ($\mathcal{H}_\infty$ norm) and in closed loop fashion ($\nu-$gap), consider the following three plants

$$P_1(s) = \frac{100}{2s+1}, \; P_2(s) = \frac{100}{2s-1}, \; P_3(s) = \frac{100}{s^2+2s+1}.$$

We observe, that $P_1, P_2$ are pretty close to each other in terms of the Bode plot for instance (see Fig. 5) and $P_3$ is quite far away from them. Obviously, the open loop behaviours of $P_1, P_2$ is quite different (as one plant is stable and the other not),. In contrast, the open loop behaviours of $P_1, P_3$ are quite similar, see Fig. 6 (left). However, the situation becomes somewhat different, when we

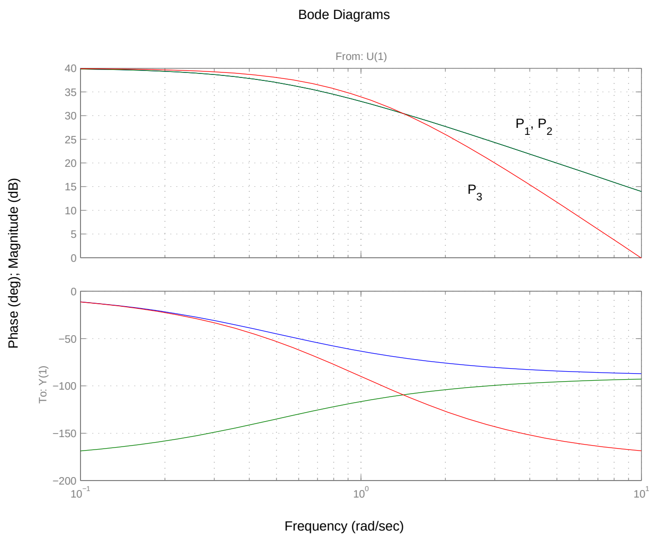


Figure 5: Bode diagrams of $P_1$ (blue), $P_2$ (green), $P_3$ (red).

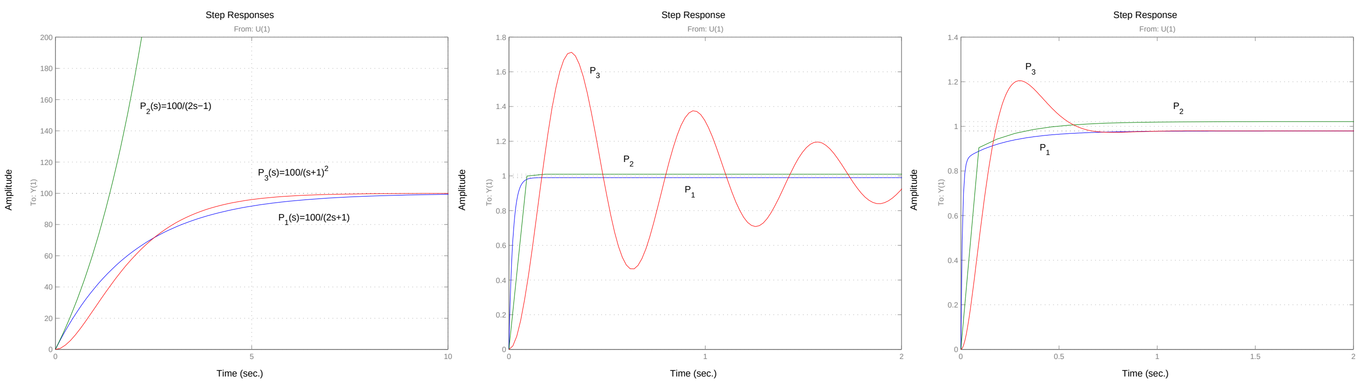


Figure 6: Step response: open loop, using controller $K = -1$, using controller $K = \frac{2.15s+11.1}{s+23.3}$ (left to right).

look at closed loop behaviour and try to control all three plants with the same controller. As visible from Fig. 6), now $P_1, P_2$ appear quite similar, while $P_3$ "fades away". This behaviour is caught when measuring the distance between the plants with $\nu-$gap and $\delta_n$ (i.e. $\mathcal{H}_\infty$-norm based) respectively. Note, that a distance close 1 in $\nu-$gap is "quite a lot".

| distance between | in $\nu-$gap-metric | in $\infty$-norm based metric |
|---|---|---|
| $P_1, P_2$ | 0.02 | 125.89 |
| $P_1, P_3$ | 0.89 | 19.95 |

### 3.4 Benefits of $\nu-$gap

To wrap up the technicalities derived so far, we state the main reasons (in order of importance) to deal with $\nu-$gap:

- In contrast to the $\mathcal{H}_2$ gap, we obtain an "if and only if" theorem for robust stability. The models too far away from the nominal one (measured in $\nu-$gap) will not be stabilised.

- $\nu -$ gap is the only metric that produces these properties
- It is easy to compute in contrast to $\mathcal{H}_2$ gap and induces the correct graph-topology (in contrast to $\mathcal{L}_2$ gap).
- It is a closed loop measure (like the other gaps) in contrast to the $\mathcal{H}_\infty$-norm.
- It automatically emphasises the cross over frequency: differences between two systems are deemed to be more serious, when they appear around crossover frequency.
- Therefore, $\nu -$ gap is useful for analysis in MIMO case, where the crossover might be difficult to detect.
- An extension of the classical $\mathcal{H}_\infty$-loop shaping design procedure is available to consider errors measured in $\nu -$ gap [25, ch.4].

# 4 Analysis of model sets with $\nu -$ gap

Rather recently, the framework stated above found its way into the "identification for control" community. Suppose, we have identified a models from data. This is, to figure out a set of model that does not contradict our observation, and a so-called nominal model. The nominal model is the best (in some sense) model describing the data we have at hand. Note, that in this stage we are independent of the actual identification philosophy. It may be a statistical framework, as well as an unkown-but-bounded framework. But stating terms like "best", we need to have some kind of measure, and, when assessing the size of the identified model set, we need a measure for this as well. Looking at for instance the volume of the geometrical object (typically ellipsoids or boxes), where the uncertain parameter is supposed to live in, does not help that much as this depends on the dimension of the parameter space (i.e. number of parameter, model order). Another way at looking at the model set "size" is plot its frequency image in either the Nyquist or the Bode plot. This approach, however, does not take care of the choosen parameterisation and especially the logarithmic scale of the Bode plot may fool the intuition about the actual size.

Motivated from the above discussion on gap-metrics and $\mathcal{H}_\infty$ norm, we observe that this way of looking at model sets is an "open loop way" anyway. Having a control application in mind, the question to be posed is more like: suppose, a controller is at hand, how far is the closed loop away from stability and certain performance requirement, accounting for *all* models in the identified model set. We motivated, that $\nu -$ gap is an easy to compute closed loop measure, that should enable such kind of analysis. This is basically the topic of [3].

What this problem boils down to, is the following scenario: Suppose a model set is identified and a controller is at hand. Is this controller robustly stable with respect to the model set? Well, in the Nyquist plane, the open loop (i.e. the model set multiplied with the controller) makes up an area, and the only question is: How far is this area away from $-1$? Including some robust performance in this context is to introduce some forbidden areas in the Nyquist plane. Note, that this argumentation is quite close to QFT notions. Surely, taking care of parameterisation issues and computability makes the actual framework more complicated, but the above picture is the one to keep in mind.

## 4.1 Robust stability issues

After the introductory motivation, we are going to introduce the notation and the formal framework. Suppose some nominal model $P_{nom}$ within a model set $\mathcal{U}$, obtained (for instance) from an identification experiment. Aiming at applying the $\nu-$ gap framework for analysing the size of this model set, the following useful distances can be introduced [3]:

**Definition 11 (Worst case chordal/Vinnicombe distance)**

- *The worst case chordal distance:*

$$\kappa_{WC}(P_{nom}(i\omega),\mathcal{U}) = \max_{P\in\mathcal{U}} \kappa(P_{nom}(i\omega), P(i\omega)) \tag{5}$$

- *The worst case Vinnicombe distance:*

$$\delta_{WC}(P_{nom},\mathcal{U}) = \max_{P\in\mathcal{U}} \delta_\nu(P_{nom}, P) \tag{6}$$

Obviously, the worst case Vinnicombe distance is the maximum over all frequencies of the worst case chordal distance (whenever the winding number condition is fulfilled). Moreover, it is useful to determine the maximum distance between the nominal model and any member of the model set: the controller will usually achieve best performance, when dealing with the nominal model. It is therefore useful to know, with what difference the robust controller might have to cope with.

Based on this definition, which is just a simple extension (see [2, th.7]) of the original ones in the above section, a sufficient condition for robust stabilisation by a *given* controller can be stated as

$$\kappa_{WC}(P_{nom}(i\omega),\mathcal{U})) < \kappa(P_{nom}(i\omega), \frac{1}{K(i\omega)}),\ \forall\omega \tag{7}$$

Some comments should be made on this methodology:

1. $\nu-$ gap delivers highly intuitive analysis results on uncertainty bands, available for instance in the frequency domain: It automatically focused on the cross-over frequency, where an as precise as possible model is asked for (in terms of controller design). However, this is already clear from intuition, and it seems that not much more can be gained (in the SISO case).

2. $\kappa_{WC}(G_{nom}(i\omega),\mathcal{U}))$ in (7) focuses "too much" on the nominal plant $G_{nom}$ in the following sense: A violation of (7) does not say anything about stability, *especially* when the controller changes the cross-over of the nominal plant. The maximum of $\kappa_{WC}(G_{nom}(i\omega),\mathcal{U}))$ appears at cross-over of the plant, not at that of the open loop. In that case, one has to weight the plant.

3. The sufficiency of the stability result given above arises from the embedding of the *identified* (parametric) uncertainty into the underlying coprime factor/graph framework.

## 4.2 Numerical solution

The formal extensions as stated above being pretty straightforward, their success will strongly depend the computability of worst case chordal or Vinnicombe distance. It turns out, that, depending on the parametrisation of $\mathcal{U}$, calculation of $\kappa_{WC}$ can be written as LMI feasibility problem (employing the $\mathcal{S}$-procedure). Suitable parametrisations for this approach include the most popular model sets, "produced" by identification methods:

- Output Error models, where the uncertain parameters are the coefficients of the two polynomials involved, living in an ellipsoid.

- Linear combination of basis functions, where the parameters again live in an ellipsoid (as a special case of the above one, so called fixed denominator models).
- Nominal (fixed) models, that come along with an explicit (additive) error model, where the error model is one the above.
- Model sets obtained via Stochastic Embedding, which is describing the uncertainty in a non-parametric way as an ellipsoid in the frequency domain fro each frequency, based on certain random walk models.

To see how LMI techniques can be applied to calculate the worst case chordal distance, we consider single-input single-output models, that are linearly parameterised, i.e. we assume the the transfer function to have the structure

$$P = B \cdot \theta$$

for the i/o behaviour, where $B$ denotes the vector of chosen basis functions, and $\theta$ the parameter vector, to be estimated from data. Doing so, we end up with a nominal model $P_{nom} = B \cdot \theta_{nom}$ and the model set:

$$\mathcal{U} \;\; := \;\; \{P(\theta);\; P(\theta) := B \cdot \theta,\; (\theta - \theta_{nom})^T E^{-1}(\theta - \theta_{nom}) \leq \rho\}. \tag{8}$$

Applying Set Membership techniques, assuming an unknown-but-bounded noise, the positive definite matrix $E$ in (8) refers to the ellipsoid, calculated when using an ellipsoidal over-bounding algorithm [16] and $\rho = 1$. Using Least Squares techniques [13], $E$ is the covariance matrix of the parameter and $\rho$ is linked to the probability level of estimation.

However, $\nu -$ gap can be used to analyse model uncertainty from our identification setup described in (8), using a similar argumentation as in [2]. In our case, however, the pointwise worst case chordal distance from the parametric uncertainty set $\mathcal{U}$ as defined in the framework above to the nominal model is given (under some cheap assumptions) by $\kappa_{WC}(P_{nom}, \mathcal{U}) = \sqrt{\gamma_{opt}}$, where $\gamma_{opt}$ is the solution of the following LMI problem:

$$\min_{\gamma,\tau}\{\gamma : 0 \leq \tau, 0 \leq \gamma, F_0 \leq \tau F_1\} \tag{9}$$

where

$$F_1 = \begin{pmatrix} R & -R\theta_{nom} \\ -\theta_{nom}^T R^T & \theta_{nom}^T R\theta_{nom} - \rho \end{pmatrix},\; F_0 = \begin{pmatrix} (1-\gamma Q)\Gamma & -\Gamma\theta_{nom} \\ -\theta_{nom}^T \Gamma & |x|^2 - \gamma Q \end{pmatrix} \tag{10}$$

denoting $x = B\theta_{nom}$, $Q = 1 + |x|^2$, $R = E^{-1}$, $\Gamma = B_R^T B_R + B_I^T B_I$ and $B = B_R + iB_I$ splits the basis function in its real and imaginary parts.

This computational framework holds, even when using an explicit and unfalsified error model of the form

$$P = P_{nom} + B\theta, \quad \theta \in \Theta \tag{11}$$

which is a special case of the model set $\mathcal{U}$ as defined in (8). For computational purposes, we employ a parameterisation of the model error model via some basis functions $B$. $\Theta$ is then the ellipsoid around the nominal value $\theta_{nom}$ for the *model error* (the nominal model error itself has no further importance). This can be derived from combining Model Error Modeling and Set Membership Estimation, see [10].

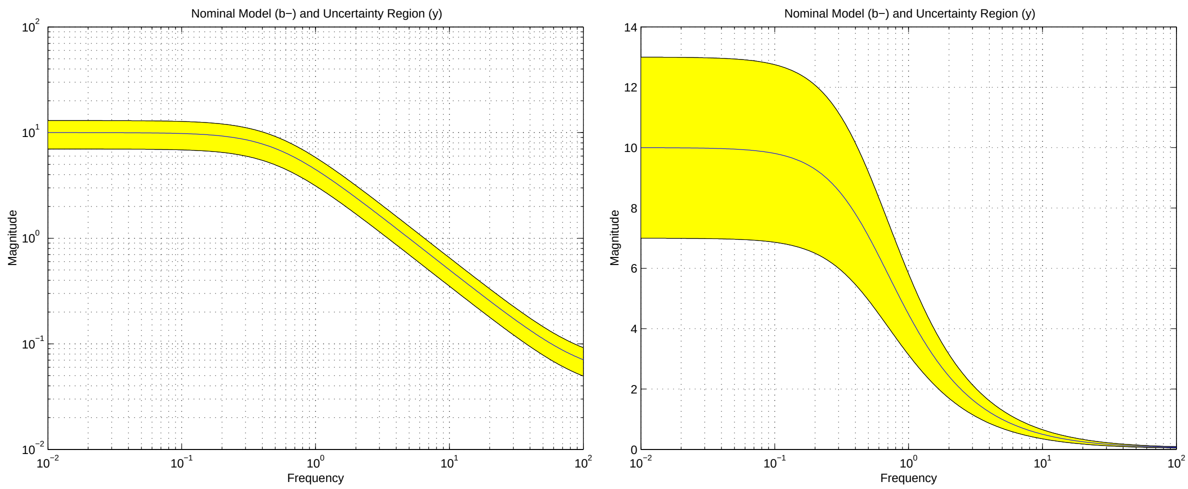


Figure 7: Nominal model (solid blue line) and its uncertainty region arising from the uncertain gain $\theta \in \Theta$ in the frequency domain: logarithmic (left) and non-logarithmic (right).

Analysing this kind of model set using $\nu-$ gap and using the same LMI optimisation as above, only one matrix has to be replaced in (9), namely:

$$F_0 = \begin{pmatrix} (1-\gamma Q)\Gamma & -(\Gamma Q(P_{nom,R}B_R + P_{nom,I}B_I) + \theta_{nom}^T\Gamma)^T \\ -(\gamma Q(G_{nom,R}B_R + P_{nom,I}B_I) + \theta_{nom}^T\Gamma) & |x|^2 - \gamma Q(1+|P_{nom}|^2) \end{pmatrix} \tag{12}$$

denoting $\Gamma = B_R^T B_R + B_I^T B_I$ and $B(s) = B_R(s) + iB_I(s)$ now the basis function used for characterisation of the *model error*. Moreover $x = P_{nom} + B\theta_{nom}$ and $Q = 1 + |x|^2$.

## 4.3 Example

Using Set Membership Estimation techniques with a basis function approach, we obtain the following (most simple) model set:

$$P(\theta, s) = \theta\frac{s+100}{s+0.5} \tag{13}$$

$$\theta \in \Theta := [0.035, 0.065] \tag{14}$$

$$\theta_{nom} = 0.05 \tag{15}$$

The setup for the identification was the choice of the basis function $B(s) = \frac{s+100}{s+0.5}$, and Set Membership Estimation on the data set gave the parameter-ellipsoid $\Theta$ (which is a simple interval in our one dimensional case), with the central estimate $\theta_{nom}$, which we think is the best estimate within this set. In fact, we are left with a first order stable and non-minimum phase system with a varying gain, where the gain lives in an interval.

We display this *parametric uncertainty* in the frequency domain (i.e. the Bode plot), which is depicted in Figure 7.

What are the difficulties from the control point of view with this model uncertainty? We therefore grid the uncertain gain $\theta$ and calculate the pointwise chordal distance of these members of the model set $P(\theta_i)$ to the nominal model $P(\theta_{nom})$, which is denoted by $\kappa(P(\theta_i), P(\theta_{nom}))$ (omitting

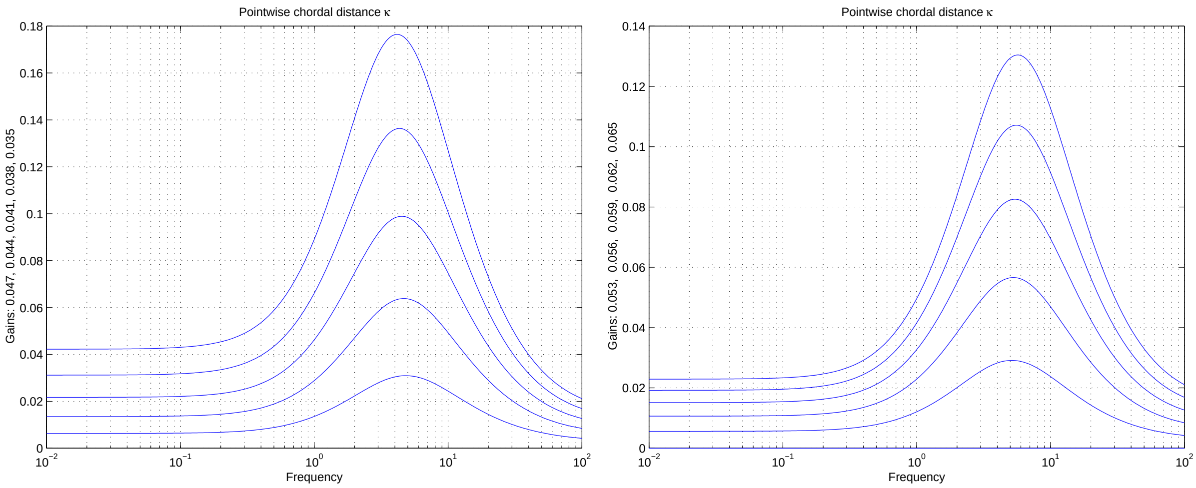


Figure 8: Pointwise chordal distance of certain members of the model set $P(\theta_i)$ to the nominal model $P(\theta_{nom})$: result for gains $\theta_i$ that are smaller and larger (respectively) than the nominal gain $\theta_{nom}$ (left and right respectively). The numerical values of the gains $\theta_i$ are indicated along the $y$-axis.

the second argument of $P$ for simplicity). The difference to the nominal model is important, because a controller design – even the design of a *robust* controller – will focus on the nominal model (which we think is the best one, derived from the knowledge we have). The robustness of the controller will take care for the uncertainties, it is therefore quite natural to ask: with what difference to the nominal model do we have to cope?

The result is depicted in Figure 8. Note, that the winding number condition is fulfilled in all cases, thus the maximum of pointwise chordal distance indicates the $\nu-$gap $\delta_\nu(P(\theta_i), P(\theta_{nom}))$. We observe, that this maximum appears around cross-over frequency: $\nu-$gap weights the difference to the nominal model more around cross-over, which makes sense from the control point of view: for a good controller design, we have to know the plant quite well in the region of the cross over frequency.

Up to now, we looked onto variations of the gain, which restricts our attention to the first order models, that are element of the uncertainty set $P(\Theta)$. Looking on the uncertainty in the frequency domain (cf. Figure 7) from the control point of view, much more systems are situated in this set, i.e. higher order systems or systems with dynamics different to the chosen basis function for the identification. Even identification procedures with an explicit error model [12, 18, 10] allow this kind of interpretation for the identified uncertainty set. We pick two members out of the model set:

$$P_7(s) = 0.04\frac{(s+0.66)(s+0.05)(s+89.06)(s^2+5.05s+8.37)(s^2+0.68s+18.94)}{(s+0.68)(s+0.47)(s+0.045)(s^2+3.25s+5.32)(s^2+0.66s+17.25)} \quad (16)$$

$$P_{lo}(s) = 0.04\frac{(s+0.07)(s+0.03)(s+2.94)(s+98.93)(s^2+0.11s+0.03)(s^2+0.05s+0.32)(s^2+31.77s+260.3)}{(s+3.11)(s+0.39)(s+0.06)(s+0.03)(s^2+0.09s+0.022)(s^2+0.05s+0.32)(s^2+30.14s+265.8)} \quad (17)$$

Theses two systems and their pointwise chordal distance to the nominal model are depicted in Figure 9. We will first explain the choice of $P_7$: As seen above, is $\nu-$gap a measure from a closed loop point of view. Differences between systems appear more significantly around crossover frequency than elsewhere. Therefore, we picked system $P_7$ with a steep descend around crossover, but otherwise within the uncertainty band. Well known from Bode's Phase-Gain relations, that this kind of system is the more difficult to control, the steeper the descent around crossover is.

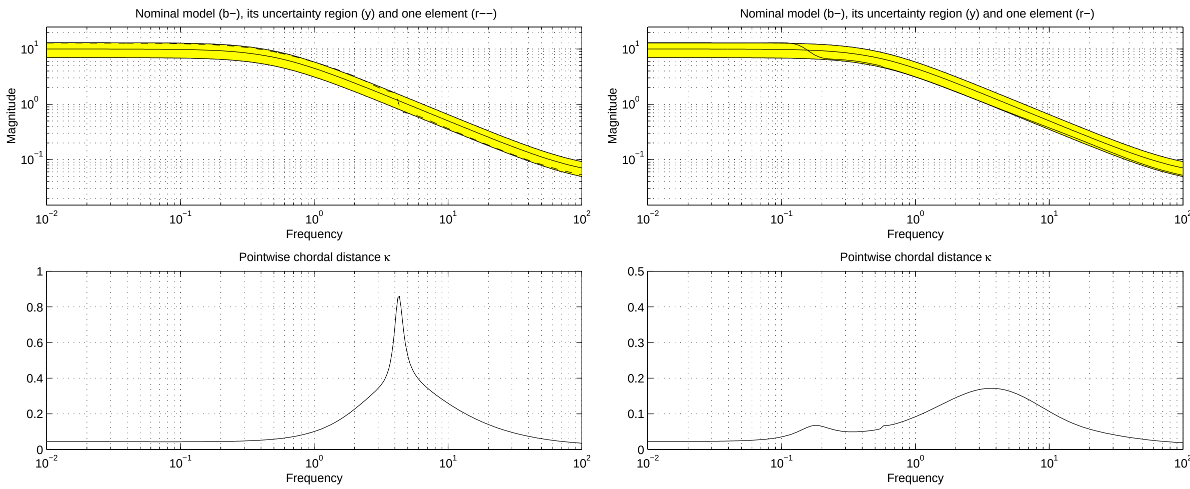


Figure 9: Upper plots: The systems $P_7$ (left) and $P_{lo}$ (right) and their location within the uncertainty set. Lower plots: Pointwise chordal distance from the nominal model $P(\theta_{nom})$ to $P_7$ (left) and $P_{lo}$ (right).

And, indeed, the pointwise chordal distance chordal distance picks this difficulty up and reached its maximum at crossover. As the winding number condition is fulfilled, this maximum is at the same time the $\nu-$gap between the two systems: $\delta_\nu(P_{nom}, P_7) = 0.8662$. Furthermore, we observe, that this $\nu-$gap is larger than the maximum $\nu-$gap to one of the model set members, which is around 0.18 (cf. Figure 8). To investigate the role of the crossover in this frequency, we do the same experiment with the system $P_{lo}$. It shows the same steep descend, but at a lower frequency, i.e. for higher gain. Visible in Figure 9 (right), that the pointwise chordal distance to the nominal model is much smaller, indeed $\delta_\nu(P_{nom}, P_{lo}) = 0.1716$ (as the winding number condition is fulfilled). In fact, the $\nu-$gap is not reached at the steep descend of the system around $\omega = 0.2$ (this is only a local maximum of the pointwise chordal distance), but at crossover! We conclude, that there are systems in the uncertainty band (possibly of higher order), with a much higher $\nu-$gap to the nominal model than the members of the model set could produce.

We continue our analysis with calculating the pointwise worst case $\nu-$gap. Using this technique, we actually calculate, for a fixed frequency, the maximum chordal distance from any member of the model set to the nominal model, which might be useful for controller design using the generalised stability margin. In this example this is, however, quite simple because of the fact that we have only one uncertain parameter, located in an interval. Nevertheless, we apply the LMI technique as stated in section 3 to solve this problem. The result is depicted in Figure 10 and coincides with the result depicted in Figure 8.

Based on the identified nominal model and the uncertainty band, we design a controller using standard $\mathcal{H}_\infty$ techniques: the controller should stabilise the uncertain gain $\theta \in \Theta$, additionally we add some second order weighting function

$$W_T(s) = \frac{20}{s^2 + 1010s + 1000} \tag{18}$$

for the complementary sensitivity function. Using LMI implementation of the $\gamma$ iteration, we obtain

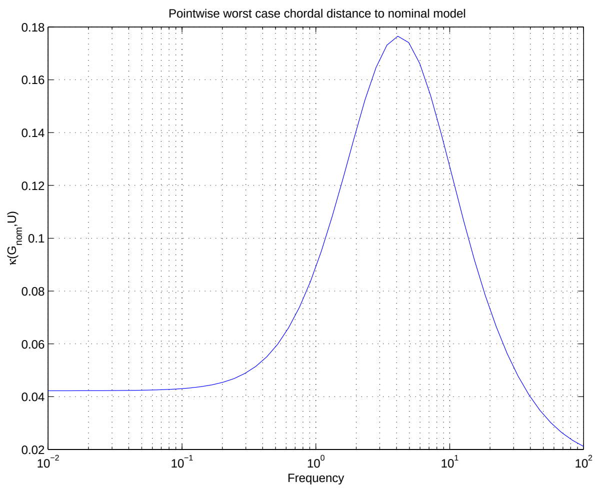


Figure 10: The pointwise worst case chordal distance from the nominal model $P(\theta_{nom})$ to the model set $P_\Theta$, calculated using LMI optimisation.

the controller

$$K_\infty = \frac{-204.6s^2 - 2.177e05s - 2.157e05}{s^3 + 1185s^2 + 1.078e05s + 1.057e05} \tag{19}$$

and the singular values of the important transfer functions of the control system are given in Figure 11. Additionally, we show in Figure 12 the control system made up with the same controller and the higher order model $[K_\infty, P_7]$, which is stabilised by the controller (by definition of the $\mathcal{H}_\infty$ control problem). We observe, that the control system $[K_\infty, P_7]$ is closer to instability (the "most right" closed loop pole located at $-0.0462$ than the nominal control system $[K_\infty, P(\theta_{nom})]$ (the "most right" closed loop pole located at $-0.9920$).

Having designed the controller we are interested in the generalised stability margin $\kappa(P_{nom}^{-1}, K_\infty)$. This is, together with the pointwise worst case chordal distance, depicted in Figure 13. As the stability margin is always larger than the worst case chordal distance, we conclude that the controller stabilises all members of the model set. But as this stability result is only sufficient, we cannot conclude the opposite: having the $\nu-$gap between nominal model and system $P_7$ of $\delta_\nu = 0.86$ appearing at frequency $\omega \approx 4$, in mind we cannot conclude that the designed controller does *not* stabilise the system (cf. Figures 13 and 9 (right)). In fact, the opposite is true and the control system $[K_\infty, P_7]$ is stable.

# 5 Ongoing research on $\nu-$gap

- Extensions of $\nu-$gap to the nonlinear case (quite a topic at CDC 1999): two different approaches so far:
  - Anderson & De Bruyne [1] and
  - Vinnicombe [24].

  Both approaches fight with some difficulties to define the winding number of systems, or, how to handle the "phase" for nonlinear systems. Thus no stability results have been derived so far.

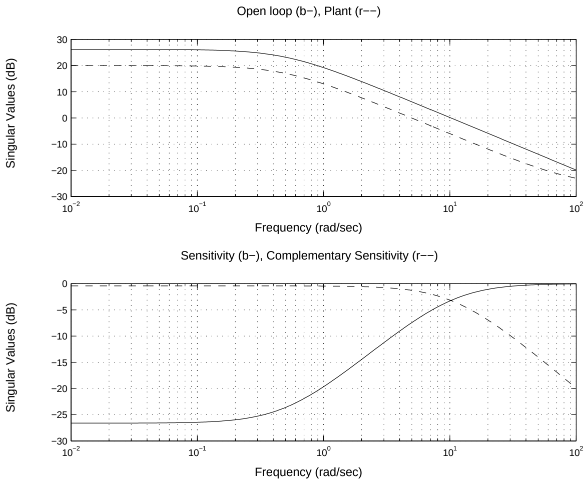


Figure 11: Singular values of plant and open loop (upper plot) and sensitivity function and complementary sensitivity function for the control system made up with controller and nominal model $[K_\infty, P(\theta_{nom})]$.

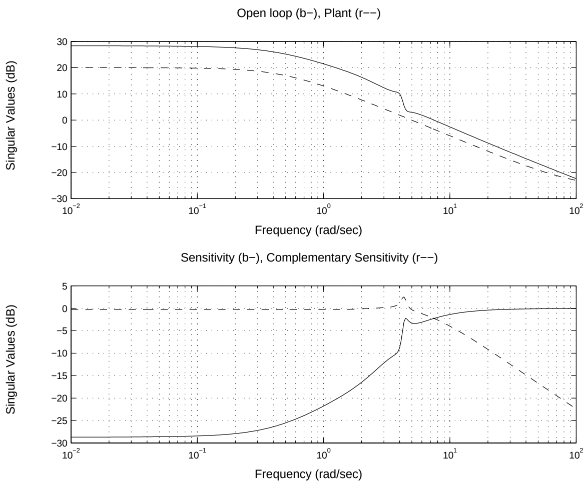


Figure 12: Singular values of plant and open loop (upper plot) and sensitivity function and complementary sensitivity function for the control system made up with controller and higher order model $[K_\infty, P_7]$.

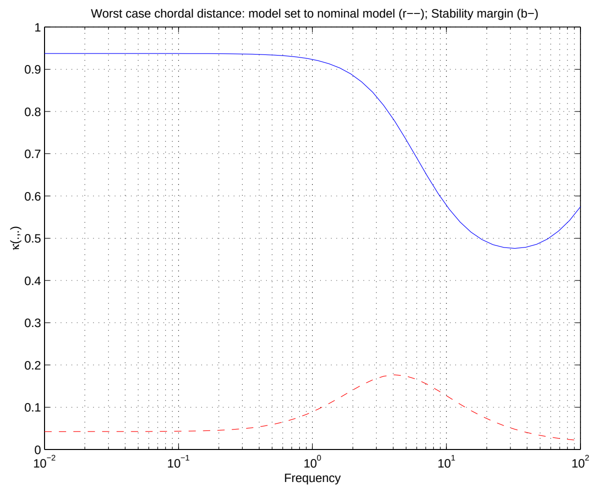


Figure 13: Pointwise worst case chordal distance from nominal model to model set (dashed red) and generalised stability margin $\kappa(P_{nom}^{-1}, K_\infty)$ (solid blue).

- For linear time varying systems, a geometric approach possible, given by Cantoni [5].
- Identification in $\nu -$ gap (P. Date): Identify (from data) a set of models, close to each other (in $\nu -$ gap sense) [6, 7, 8, 9].
- However, in the identification for control context $\nu -$ gap seems more like an analysis tool rather than a design tool (for robust controllers). The bottom line of this analysis is always, that a precise model is needed around the intended crossover frequency. Recent works on analysis [4] and controller design [19] therefore use necessary and sufficient robust stability results, based on the stability radius for rank one uncertainties [15].

## Acknowledgement

This work was supported by the European Commission through the program Training and Mobility of Researchers - Research Networks and through the project System Identification (FMRX CT98 0206). Contacts and discussions with the participants in the European Research Network System Identification (ERNSI) are gratefully acknowledged. Especially Paresh Date and Xavier Bombois have been very co-operative and patient in answering questions. Many discussions with Lennart Ljung on sausages in the Nyquist plane and related things have been extremely helpful (and enjoyable!) to get the correct picture and intuition of the technical framework described here.

## References

[1] B. D. O. Anderson and F. D. Bruyne. On a nonlinear generalization of the $\nu$-gap metric. In *Proc. of the 38th IEEE Conference on Decision and Control*, pages 3851–3856, Phoenix, AZ, USA, Dec. 1999.

[2] X. Bombois, M. Gevers, and G. Scorletti. Controller validation based on an identified model. In *Proc. of the 38th IEEE Conference on Decision and Control*, pages 2816–2821, Phoenix, AZ, USA, Dec. 1999.

[3] X. Bombois, M. Gevers, and G. Scorletti. A measure of robust stability for an identified set of parametrized transfer functions. *IEEE Trans. on Automatic Control*, 45(11):2141–2145, Nov. 2000.

[4] X. Bombois, M. Gevers, G. Scorletti, and B. D. O. Anderson. Controller validation for stability and performance based on an uncertainty region designed from an identified model. In *Proc. of the System Identification Symposium SYSID*, Santa Barbara, CA, USA, June 2000.

[5] M. Cantoni. Gap metric performance bounds for linear feedback systems. In *Proc. of the 38th IEEE Conference on Decision and Control*, pages 4505–4510, Phoenix, AZ, USA, Dec. 1999.

[6] P. Date. *Identification for Control: Deterministic Algorithms and Error Bounds.* PhD thesis, Dept of Engineering, University of Cambridge, Cambridge CB2 1PZ, UK, 2000.

[7] P. Date and G. Vinnicombe. New untuned algorithms for worst case identification. In *Proc. of the 37th IEEE Conference on Decision and Control*, pages 1281–1286, Tampa, FL, USA, Dec. 1998.

[8] P. Date and G. Vinnicombe. An algorithm for identification in the $\nu$-gap metric. In *Proc. of the 38th IEEE Conference on Decision and Control*, pages 3230–3235, Phoenix, AZ, USA, Dec. 1999.

[9] P. Date and G. Vinnicombe. Worst case identification using FIR MOdels. In *Proc. of the European Control Conference*, Karlsruhe, Germany, Aug. 1999.

[10] A. Garulli and W. Reinelt. On model error modeling in set membership identification. In *Proc. of the System Identification Symposium SYSID*, pages WeMD1–3, Santa Barbara, CA, USA, June 2000.

[11] M. Green and D. J. N. Limebeer. *Linear Robust Control.* Prentice Hall, Englewood Cliffs, NJ, USA, 1995.

[12] L. Ljung. Model validation and model error modeling. In B. Wittenmark and A. Rantzer, editors, *Proc. of the Åström Symposium on Control*, pages 15–42, Lund, Sweden, Aug. 1999. Studentliteratur, Lund, Sweden.

[13] L. Ljung. *System Identification – Theory For the User.* Prentice Hall, Upper Saddle River, NJ, USA, 2nd edition, 1999.

[14] D. C. McFarlane and K. Glover. *Robust Controller Design Using Normalized Coprime Factor Plant Description.* Number 138 in Lecture Notes in Control and Information Science. Springer Verlag, Berlin, Germany, 1989.

[15] A. Megretski and A. Rantzer. System analysis via Integral Quadratic Constraints. *IEEE Trans. on Automatic Control*, 47(6):819–830, June 1997.

[16] M. Milanese, J. P. Norton, H. Piet-Lahanier, and E. Walter, editors. *Bounding Approaches to System Identification.* Plenum Press, New York, NY, USA, 1996.

[17] P.-O. Nyman. Multidirectional optimal robustness under gap and coprime factor uncertainties. In *Proc. of the 38th IEEE Conference on Decision and Control*, pages 3617–3620, Phoenix, AZ, USA, Dec. 1999.

[18] W. Reinelt, A. Garulli, L. Ljung, J. H. Braslavsky, and A. Vicino. Model error concepts in identification for control. In *Proc. of the 38th IEEE Conference on Decision and Control*, pages 1488–1493, Phoenix, AZ, USA, Dec. 1999. Invited Session.

[19] W. Reinelt and L. Ljung. Robust control of identified models with mixed parametric and non-parametric uncertainties. In *Proc. of the European Control Conference*, Porto, Portugal, Sept. 2001.

[20] M. Vidyasagar. *Control System Synthesis - A Factorization Approach*. MIT Press, Cambridge, MA, USA, 1985.

[21] G. Vinnicombe. Frequency domain uncertainty and the graph topology. *IEEE Trans. on Automatic Control*, 38(9):1371–1383, Sept. 1993.

[22] G. Vinnicombe. *Measuring the Robustness of Feedback Systems*. PhD thesis, Dept of Engineering, University of Cambridge, Cambridge CB2 1PZ, UK, 1993.

[23] G. Vinnicombe. The robustness of feedback systems with bounded complexity controllers. *IEEE Trans. on Automatic Control*, 41(6):795–803, June 1996.

[24] G. Vinnicombe. A $\nu$-gap distance for uncertain and nonlinear systems. In *Proc. of the 38th IEEE Conference on Decision and Control*, pages 2557–2562, Phoenix, AZ, USA, Dec. 1999.

[25] G. Vinnicombe. *Uncertainty and Feedback ($H_\infty$ loop shaping and the $\nu$-gap metric)*. Imperial College Press, London, UK, 1st edition, 2000.

[26] K. Zhou and J. C. Doyle. *Essentials of Robust Control*. Prentice Hall, Upper Saddle River, NJ, USA, 1998.

[27] K. Zhou, J. C. Doyle, and K. Glover. *Robust and Optimal Control*. Prentice Hall, Upper Saddle River, NJ, USA, 1996.